Bulgarian Journal of Physics vol. **48** (2021) 467–474

The Influence of Triaxial Deformation and Quasiparticle Alignment on the Structure of Chiral Partner Bands

R. Budaca

"Horia Hulubei" National Institute for Physics and Nuclear Engineering,
Str. Reactorului 30, RO-077125, POB-MG6 Bucharest-Măgurele, Romania

Received *9 October 2021*

Abstract. The chiral partner bands are investigated within a semiclassical treatment of a particle-rotor Hamiltonian with rigid quasiparticle alignments. The study focuses on the variation of spectral characteristics and associated dynamics inferred by considering different triaxial deformation of the core or non-axial quasiparticle alignments with arbitrary tilting. The analysis is performed for a valence $h_{11/2}$ particle and $h_{11/2}$ or $g_{9/2}$ hole alignments. As a result, distinct dynamical characteristics are identified in specific angular momentum ranges, especially concerning the chiral vibration regime.

KEY WORDS: Chiral bands, particle-rotor model, semiclassical description.

1 Introduction

A system of three mutually perpendicular angular momentum vectors can form two trihedral corners encompassing the total angular momentum vector and having opposite intrinsic handedness or chirality associated with a clockwise or counter-clockwise evolution of the principal axes ordering. Such a chiral geometry was initially suggested for odd-odd nuclei [1], where the three vectors come from the rotation of the even-even triaxial core and of the two quasiparticles with opposite particle-hole features. The fingerprint of chiral alignment in nuclei is the existence of a degenerated doublet of rotational bands with the same parity which emerge due to the restoration of the chiral symmetry. The variety of spectral characteristics displayed by the observed chiral partner bands in over 40 nuclei [2], suggests that this is a highly idealized picture. Indeed, the degeneracy of states in the identified chiral bands is rarely encountered, while the perfect trihedral alignment cannot be maintained along the whole bands. In order to explain some features of the chiral bands' evolution with spin, one will

review here the effects of triaxial deformation [3] and of non-axial quasiparticle alignments [4] on the dynamics of a fixed three vector system.

2 Theoretical Formalism

As in the other theoretical studies of chiral bands, the particle-rotor model [5] is the starting point. A tractable semiclassical treatment of the two quasiparticles plus core system requires a frozen alignment approximation for the quasiparticle spins. Here one considers that the two quasiparticle spins are fixed in the principal planes 1-3 and 2-3, with their direction specified by the tilting angles α and α' [4]:

$$\begin{aligned} \hat{j}_1 &= j_1 \cos\alpha\,, \quad & \hat{j'}_1 &= 0\,, \\ \hat{j}_2 &= 0\,, & \hat{j'}_2 &= j' \cos\alpha'\,, \\ \hat{j}_3 &= j \sin\alpha\,, & \hat{j'}_3 &= j' \sin\alpha'\,. \end{aligned} \tag{1}$$

The triaxial core is considered as having the maximal moment of inertia along the third axis. If one considers the hydrodynamic model for the moments of inertia

$$\mathcal{J}_k = \frac{4}{3}\mathcal{J}_0 \sin^2\left(\gamma - \frac{2}{3}k\pi\right), \tag{2}$$

the triaxial deformation should then be restricted to the interval $\gamma \in (60^\circ, 120^\circ)$. $\mathcal{J}_0$ contains in principle the dependence on axial deformation β, but in the present approach it acts only as a scaling constant.

The relevant part of the particle-rotor Hamiltonian with only the total angular momentum components as acting operators is dequantized through a variational principle with a coherent state for angular momentum operators [3,4,6–9] with axis 3 chosen as a quantization axis. The later is parametrized within a stereographic representation of the total angular momentum vector, which provides a pair of canonical coordinates - the azimuth angle φ and the third axis projection $x = I\cos\theta$ of the total spin vector. x is referred to as a chiral variable, because it changes its sign when the handedness of the system changes due to the inversion of the core rotation direction. The classical energy function obtained from the variational principle is expressed in terms of the canonical variables as:

$$\begin{aligned} \mathcal{H}(x,\varphi) = {} & \frac{I}{2}(A_1 + A_2) + A_3 I^2 \\ & + \frac{(2I-1)(I^2-x^2)}{2I}(A_1\cos^2\varphi + A_2\sin^2\varphi - A_3) \\ & - 2\sqrt{I^2-x^2}(A_1 j\cos\alpha\cos\varphi + A_2 j'\cos\alpha'\sin\varphi) \\ & - 2A_3 x(j\sin\alpha + j'\sin\alpha'). \end{aligned} \tag{3}$$

Here, $A_k = 1/(2\mathcal{J}_k)$ are inertial parameters. The classical energy function can have one or two minima along the chiral variable x when the shape is restricted

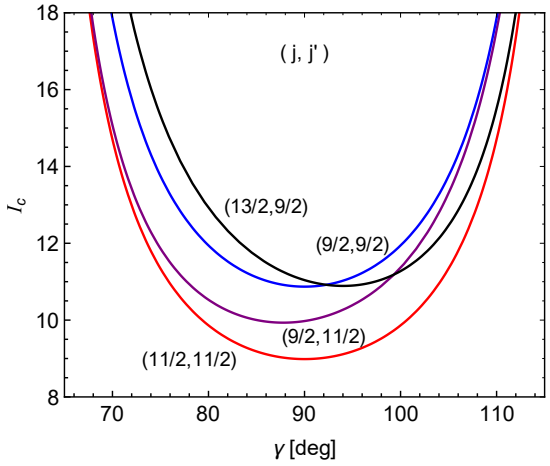

Figure 1. (Color online) The evolution as a function of triaxiality γ of the separatrix represented by the critical angular momentum I_c for a few quasiparticle configurations known to generate chiral bands.

to $\gamma \in (60^\circ, 120^\circ)$. The single minimum describes the planar solution corresponding to the chiral vibration, where the most favorable direction of the total angular momentum lies in the principal plane defined by the two axially aligned quasiparticles. As the total angular momentum increases, the single minimum splits into two configurations associated with static chirality, where the angular momentum direction favors two aplanar orientations. When there is no tilting, the two aplanar configurations are equivalent in what concerns the energy cost. The transition takes place from planar to aplanar phase with the increase of angular momentum. As can be seen from Figure 1, the critical angular momentum where this transition takes place is higher with the loss of triaxiality. Similarly, Figure 2 shows that the higher energy second minimum in the tilted alignment configuration appears sooner for small tilting, with the critical angular momentum reaching a saturation for moderate tilting.

To this classical function, one can associate a quantum Hamiltonian:

$$\hat{H}_c = -\frac{1}{2}\frac{1}{\sqrt{B(x)}}\frac{d}{dx}\frac{1}{\sqrt{B(x)}}\frac{d}{dx} + V(x), \tag{4}$$

where

$$B(x) = \left[\frac{\partial^2 \mathcal{H}(x,\varphi)}{\partial \varphi^2}\right]^{-1}_{\varphi_0(x)}, \tag{5}$$

$$V(x) = \mathcal{H}(x,\varphi_0(x)) + \frac{B''(x)}{8\left[B(x)\right]^2} - \frac{9\left[B'(x)\right]^2}{32\left[B(x)\right]^3}, \tag{6}$$

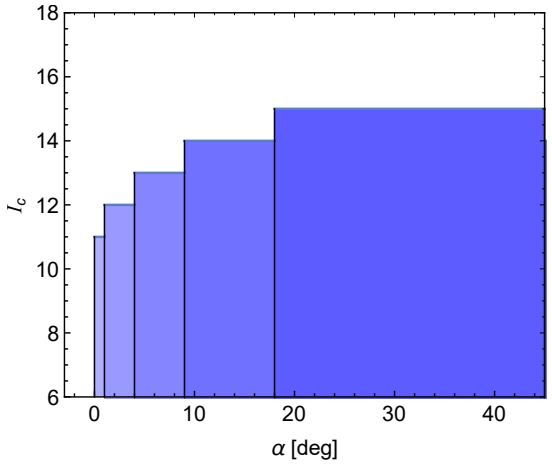

Figure 2. (Color online) The tilting angle $\alpha = \alpha'$ intervals valid for the same critical integer values of the total angular momentum up to which the classical energy function exhibits a single minimum for the $j = j' = 11/2$ configuration.

are the coordinate-dependent effective mass and the chiral potential. $\varphi_0(x)$ is the minimal value of the azimuth angle for a fixed chiral variable x, which is used in approximating the classical energy function as second order expansion only in the φ variable:

$$\tilde{\mathcal{H}}(x,\varphi) \approx \mathcal{H}(x,\varphi_0(x)) + \frac{1}{2}\left(\frac{\partial^2 \mathcal{H}}{\partial \varphi^2}\right)_{\varphi_0(x)} \left(\varphi - \varphi_0(x)\right)^2 . \tag{7}$$

With this, one can retain the information about the chiral variable. The quantum Hamiltonian (4) is then obtained from (7) by the correspondence $\varphi = i\frac{d}{dx}$. Note that x plays the role of a classical generalized momentum, and the performed quantization is equivalent to working in the momentum space. It is then evident that the above harmonic approximation is actually needed for the separation of the kinetic and potential energies. When $\gamma = 90^\circ$ and $A_1 = A_2$, the φ_0 angle becomes constant $\varphi_0 = \frac{j' \cos\alpha'}{j \cos\alpha}$ and one can use directly $\varphi - \varphi_0 = i\frac{d}{dx}$ for the quantization procedure. Otherwise, it must be determined numerically from a quartic equation in $\cos\varphi_0(x)$ or $\sin\varphi_0(x)$ for each angular momentum value. The quantum Hamiltonian is diagonalized in a basis of particle in the box wave-functions, because the problem is naturally bounded by $|x| \leq 1$.

3 Numerical Examples

From the geometry of the considered system, one can see that the low spin states are characterized by an average direction of the total angular momentum vector

confined to the plane defined by the two quasiparticle alignments. It can execute fluctuations around this equilibrium direction, defining thus the so called chiral vibration regime. As the total and core angular momentum increases, this fluctuation raises in amplitude and eventually two tilted orientations of the total angular momentum vector in respect to the quasiparticle plane become more favorable. Note that this is not yet the end of the chiral vibration phase, because the fluctuation around the quasiparticle plane is still possible albeit in a double minimum regime with and without quantum tunneling effects. Only when the two possible directions of the total angular momentum on the opposite sides of the quasiparticle plane no longer interact, one obtains the static chirality and the expected minimal energy split between the corresponding states. If the two chiral directions are equivalent, the high spin states become degenerate. Otherwise, there will be an energy split reflecting the energetic advantage of one static configuration over the other. The evolution of the quantum energy split between the partner bands is consistent with this dynamical picture.

First, considering the axial alignments of the quasiparticle spins, one can see from Figure 3 that the two bands indeed reach a degeneracy at high spins, where the two static geometries are equivalent and the states are symmetric and antisymmetric combinations of right and left handed solutions. The angular momentum where degeneracy commences depends on both quasiparticle spins and the

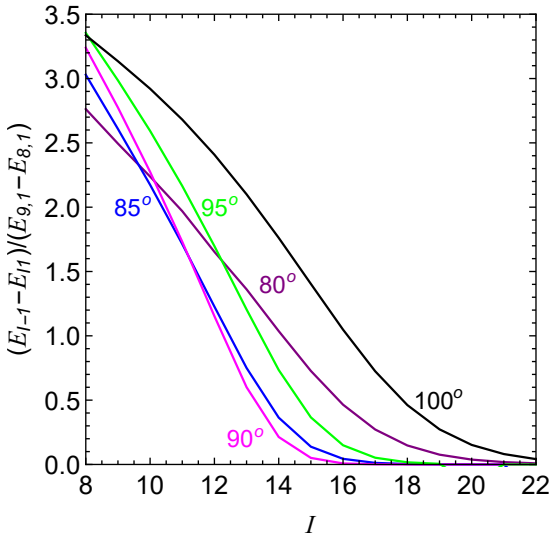

Figure 3. (Color online) Evolution with angular momentum of the energy difference between the same angular momentum states of the two chiral bands for $j = 9/2$, $j' = 11/2$ and different triaxial deformation γ. The energies are given in respect to the lowest considered state 8^+ and normalized to the first excitation energy from the yrast state.

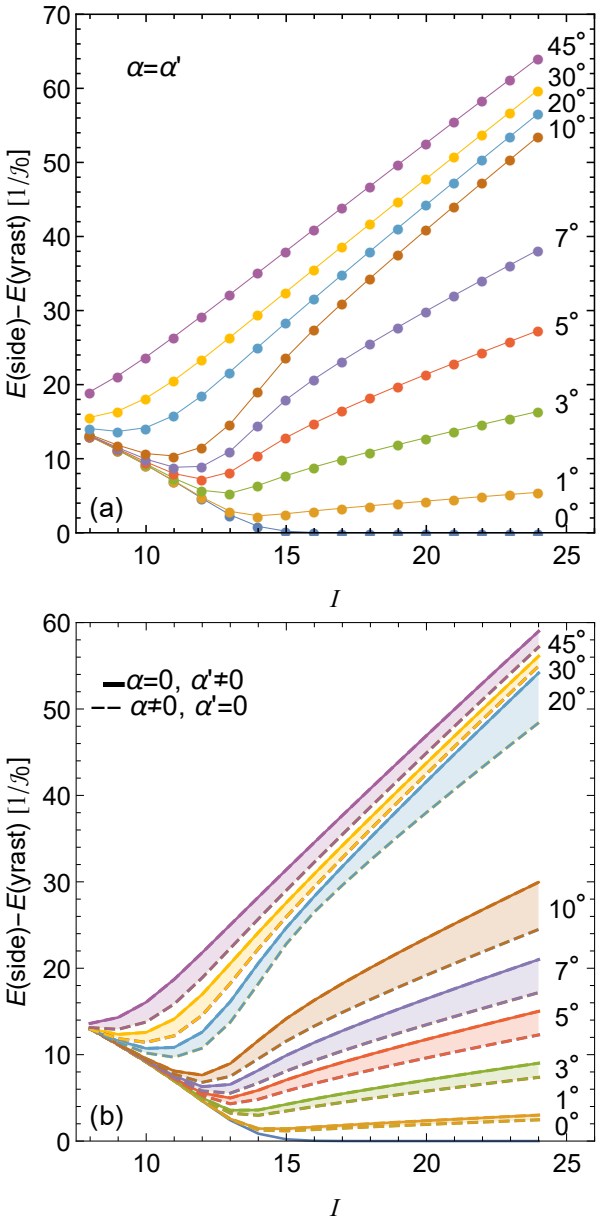

Figure 4. (Color online) Theoretical energy differences between the partner bands as a function of angular momentum and for different tilting $\alpha = \alpha'$ (a) and $\alpha(\alpha') \neq 0$ (b) of the quasiparticle spins $j = 9/2$ and $j' = 11/2$.

triaxial deformation. For example, in comparison to the previous $j = j' = 11/2$ results [3, 4, 9], the point of degeneracy is slightly shortened for the $j = 9/2$ and $j' = 11/2$ case. Moreover, due to $j \neq j'$, the prolate and oblate results are no longer equal. In general, by decreasing the triaxiality towards a more axially symmetric shape, the onset of degeneracy is forestalled. This change is different for the decrease of triaxiality toward prolate or ablate shapes when $j \neq j'$. Figure 3 shows that for the oblate-like shapes the energy difference has initially just a smaller decreasing slope, while for the prolate branch of deformations, the dependence on total spin of the energy difference is overall shifted to higher values.

In what follows, one will discuss the effect of non-axial quasiparticle alignments only for the case with maximal triaxiality $\gamma = 90^\circ$ which significantly simplifies the calculations. As was revealed in Ref. [4], any tilting of the quasiparticle spins leads to the loss of the energy degeneracy expected at high spin states. This feature can be seen in Figure 4, from where one also observes that the angular momentum where the degeneracy of partner bands starts in the axial alignment case becomes a minimum after which the energy difference has a steady increase with spin. As the tilting of the quasiparticle spins plane increases, this energy difference minimum shifts to lower spin values and the afterward slope of spin-dependence increases. At extreme tilting, the minimum disappears from the energy difference, which becomes a monotonically increasing function of angular momentum. This behaviour reminds of the wobbling energy in the simple even-even triaxial rotor [5]. As a matter of fact, for a sufficient tilting of the quasiparticle alignments, the excited state shifts from acting as a "ground state" in the higher energy chiral configuration to being an excited state in the same minimal energy configuration as the ground state. In the regime of small tilting, each high spin state is localized in one of the energy minima, having thus well-defined chirality. This situation is different from the static chirality in the perfect trihedral geometry, where the two states are superposition of states with opposite chirality. Basically, one still have a dynamical transition from chiral vibration to one of the discussed scenarios, depending on the degree of tilting.

The calculations performed in Ref. [4] for the case of $j = j' = 11/2$ provided more or less the same results for different combinations of tilting angles $\alpha + \alpha' = const.$ However, considering different hole and particle spins $j \neq j'$, leads to a more significant variation in spin dependence of the energy difference between bands as a function of different tilting combinations $\alpha+\alpha'$. Indeed from Figure 4(b), one can observe that the difference between results corresponding to the tilting of only one quasiparticle is significant, especially for moderate angles and at higher spin values.

4 Conclusions

Using the semiclassical description of Refs. [3, 4, 9], one showed that deviations from maximal triaxiality of the core as well as from the principal axes alignments of the quasiparticle spins are responsible for the loss of energy degeneracy at high spin states. On one hand, lower triaxiality maintains the chiral vibration regime up to very high spins. On the other hand, even small quasiparticle alignment deviations from principal axes generate a non-vanishing energy shift between the two configurations with opposite handedness. Moreover, important changes to the system's dynamics take place in specific intervals of angular momentum as a function of tilting angles, involving dynamical regimes such as asymmetric chiral vibration, rotations along two distinct directions with well-defined handedness and tilted-axis wobbling behaviour. As a future project one envisages the application of this model to wobbling bands in odd and even mass nuclei.

Acknowledgements

This work was supported by project PN-19-06-01-01/2019-2022 of the Ministry of Research, Innovation and Digitalization, Romania.

References

[1] S. Frauendorf, J. Meng (1997) Tilted rotation of triaxial nuclei. *Nucl. Phys. A* **617** 131. DOI: https://doi.org/10.1016/S0375-9474(97)00004-3.

[2] B. W. Xiong, Y. Y. Wang (2019) Nuclear chiral doublet bands data tables *At. Data Nucl. Data Tables* **125** 193. DOI: https://doi.org/10.1016/j.adt.2018.05.002.

[3] R. Budaca (2019) Role of triaxiality in the structure of chiral partner bands. *Phys. Lett. B* **797** 134853. DOI: https://doi.org/10.1016/j.physletb.2019.134853.

[4] R. Budaca (2021) From chiral vibration to tilted-axis wobbling within broken chiral symmetry. *Phys. Lett. B* **817** 136308. DOI: https://doi.org/10.1016/j.physletb.2021.136308.

[5] A. Bohr, B. R. Mottelson (1975) "*Nuclear Structure, vol. 2*". Benjamin, Reading, Massachusetts.

[6] A.A. Raduta, R. Budaca, C.M. Raduta (2007) Semiclassical description of a triaxial rigid rotor. *Phys. Rev. C* **76** 064309. DOI: https://doi.org/10.1103/PhysRevC.76.064309.

[7] R. Budaca (2018) Tilted-axis wobbling in odd-mass nuclei. *Phys. Rev. C* **97** 024302. DOI: https://doi.org/10.1103/PhysRevC.97.024302.

[8] R. Budaca (2021) Reconciliation of wobbling motion with rotational alignment in odd mass nuclei. *Phys. Rev. C* **103** 044312. DOI: https://doi.org/10.1103/PhysRevC.103.044312.

[9] R. Budaca (2018) Semiclassical description of chiral geometry in triaxial nuclei. *Phys. Rev. C* **98** 014303. DOI: https://doi.org/10.1103/PhysRevC.98.014303.